

Supporting Information

Carbohydrate-based surfactants as photocontrollable inhibitors of ice recrystallization.

Madeleine K. Adam,^a Jessica S. Poisson,^a Yingxue Hu,^b Geethika
Prasannakumar,^b Matthew J Pottage,^b Robert N. Ben^{*a} and Brendan L.
Wilkinson^{*b,c}

a) Department of Chemistry, 10 Marie Curie, University of Ottawa, Ontario, Canada K1N 6N5

b) School of Chemistry, Monash University, Victoria 3800, Australia

c) School of Science and Technology, The University of New England, New South Wales
2351, Australia

Table of Contents

1.0 Materials and Methods	3
General	3
Surface tension measurements	4
UV-Vis spectroscopy	4
Octanol/water partition coefficient (Log P)	6
Ice Recrystallization Inhibition (IRI) Assay	9
Quantitative Analysis of Ice Recrystallization Inhibition (IRI)	10
Thermal Hysteresis (TH) Assay	10
Cryopreservation of Tf-1 α cells	11
Toxicity Experiments with ManAzo 2 (30 mM)	15
2.0 Synthesis and analytical data	17
3.0 References	29

1.0 Materials and Methods

General

Analytical thin layer chromatography (TLC) was performed on commercially prepared silica plates (Merck Kieselgel 60 0.25 mm F254). Flash column chromatography was performed using 230-400 mesh Kieselgel 60 silica eluting with distilled solvents as described. Solvents and reagents were purchased from Sigma-Aldrich and Merck and used without further purification. ^1H NMR and ^{13}C NMR spectra were recorded on a Bruker Avance 400 NMR spectrometer at frequencies of 400 MHz and 100 MHz respectively. Chemical shift is reported as parts per million (ppm) downfield shift. The data are reported as chemical shift (δ), multiplicity, relative integral, coupling constant ($J = \text{Hz}$) and assignment where possible. IR spectra were recorded on a Bruker ATR spectrometer. Optical rotation was measured on an Optical Activity Polaer 2001 (546 nm) polarimeter using a 1 mL cell.

LC-MS was recorded on an Agilent 6120 LC-MS system operating in positive ion mode. Separations were performed on an Agilent Poroshell-120 2.7 μm (3.0 mm x 50 mm) C18 column using a linear gradient of 0.1% formic acid in water (Solvent A) and 0.1% formic acid in acetonitrile (Solvent B) as the mobile phase. Separations were performed using a linear gradient of 20% solvent B to 100% solvent B over 15 minutes, operating at a flow rate of 0.3 mL/min.

Deprotected carbohydrate-based surfactants **1-3**, were purified by reversed-phase (C18) preparative HPLC using an Agilent 1260 preparative HPLC system equipped with an automated fraction collector. Separations were performed on an Agilent Zorbax SB300 5 μm (20 mm x 150 mm) C18 column using a linear gradient of 0.1% formic acid in water (Solvent A) and 0.1% formic acid in acetonitrile (Solvent B) as mobile phase, operating at a flow rate of 10 mL/min. Surfactants **1-3** were purified using a linear gradient of 20% solvent B to 100% solvent B over 40 minutes (monitoring at 280 nm). Purified

fractions were subsequently combined and lyophilized.

Surface tension measurements

Surface tension measurements were made on a custom-designed pendant drop instrument.¹ A time series was taken (that is, surface tension as a function of time) and values were noted for 100 s to ensure full equilibration of interfacial adsorption. Once a stable surface tension had been attained, this was recorded. Drop volumes were measured throughout and changes of <5% throughout the course of a measurement were a requirement for the data shown. Critical micelle concentration (CMC) values were obtained from the intersection of lines extrapolated from surface tension values in the near pre- and post-CMC regions (Figure S3).

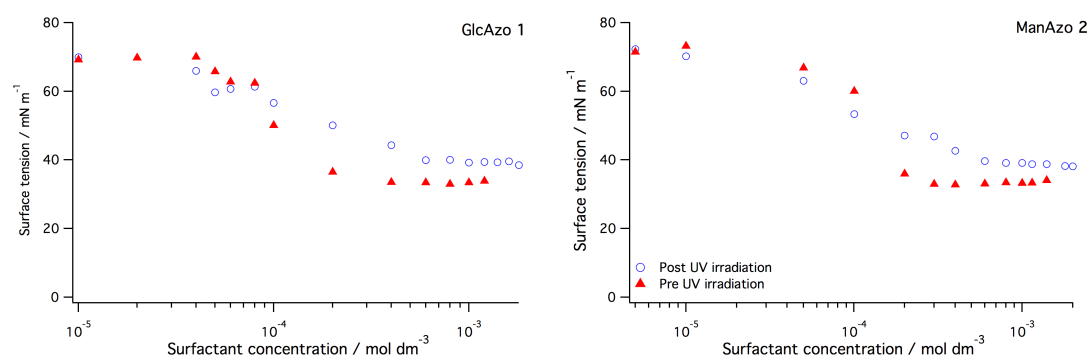


Figure S1. Photocontrollable surface tension data for GlcAzo **1** and ManAzo **2**.

UV-Vis spectroscopy

UV-visible spectroscopy was performed using a Cary 60 spectrophotometer. The molar extinction coefficients of the two main peaks, at roughly 450 nm and 350 nm in the samples in each photo-stationary state, were calculated for samples 1, 2 and 3 *via* analysis of five samples with a concentration ratio of 1:2:3:4:5, where the absorbance of the most concentrated sample was just below 1.0 to ensure the applicability of the Beer-Lambert law. In the photoillumination experiments, the *trans*-dominated and the *cis*-dominated spectra were taken from samples immediately after dilution and after 10 minutes of irradiation under a fluorescent tube lamp (peak wavelength 361

nm, 6.5 W radiant power). The ratio of molecules in the *cis* and *trans* dominated photostationary states were estimated by integration of the resolved methylene proton of the *n*-butyl group in the ^1H NMR spectrum of ManAzo **2** (Figure S2).

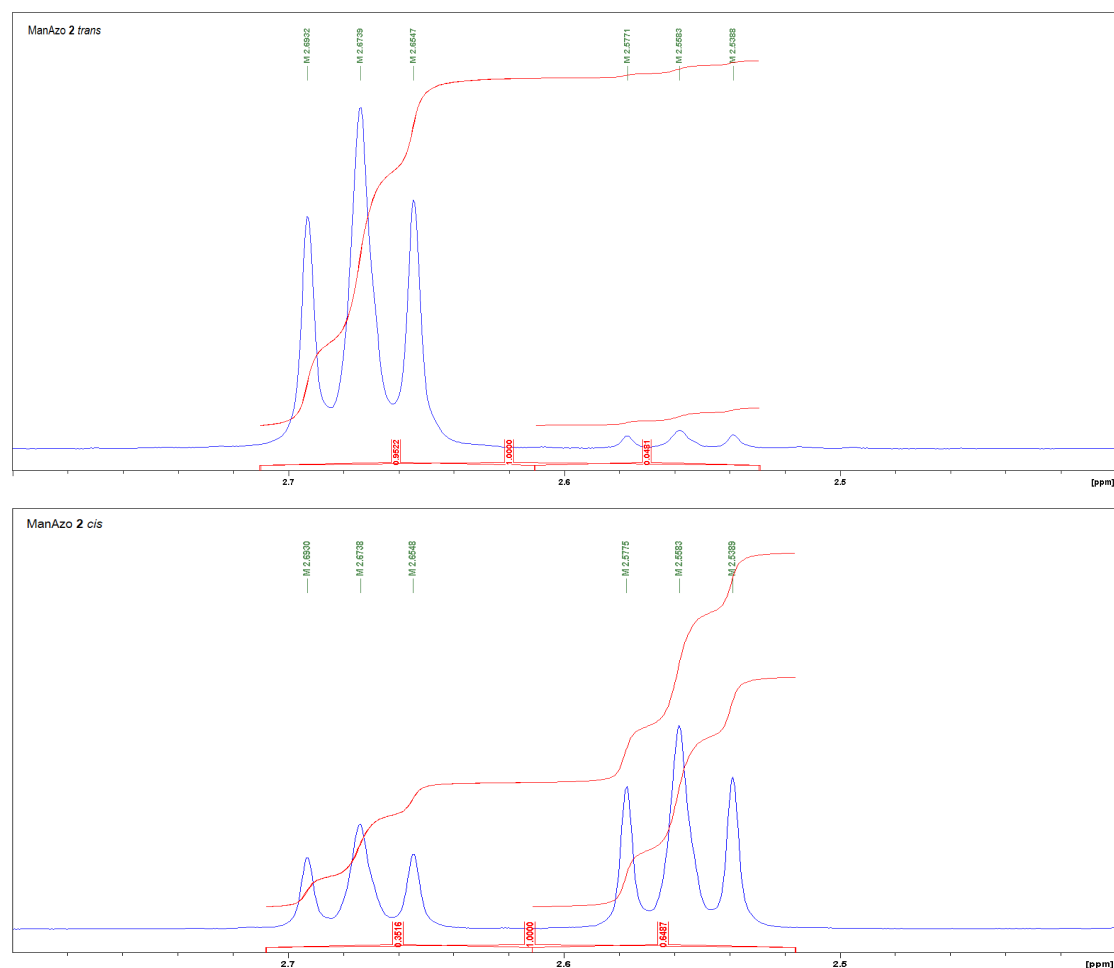


Figure S2. Expanded ^1H NMR spectrum of ManAzo **2** (20 mM in CD_3OD) in the *trans*-dominated state (top) and the *cis*-dominated state (bottom).

The native *trans* isomers of **1-3** were converted into *cis* states by illumination of their aqueous solutions under ambient conditions using a UV lamp with λ_{max} at 361 nm for 10 minutes, although one minute of photoexcitation was found sufficient to convert *trans* isomers into *cis* state. The native *trans* isomers remained stable under ambient lighting conditions at least up to 24 h, as evident from insignificant changes in their UV-vis absorbance spectra over this period. The thermal relaxation studies were performed in dark adapted

conditions at ambient temperature (approximately 20 °C). The half-lives of the *cis* isomers in water estimated by plotting the ratios of peak area under 350 nm peak and that under 440 nm peak over a period of 24 h (**Figure S3**). These peaks were chosen as *cis-trans* relaxation results in increase in peak intensity at ~350 nm, with corresponding decrease in peak intensity at 440 nm.

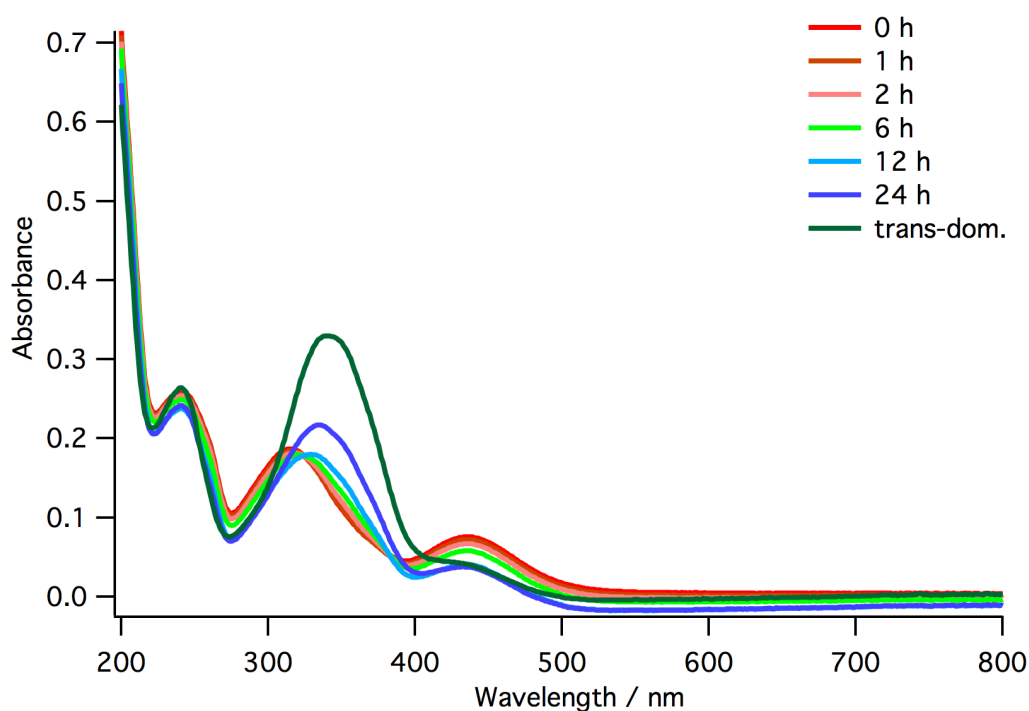


Figure S3. Thermal relaxation of *cis* ManAzo **2** over 24 hours.

Octanol/water partition coefficient (Log P)

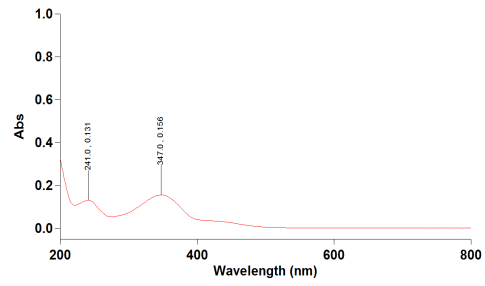
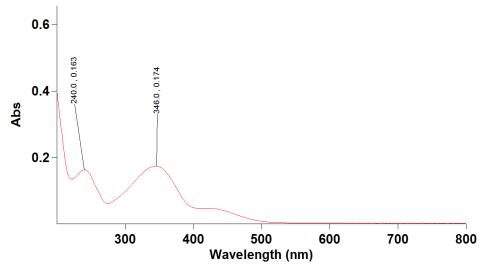
The log *P* of surfactants was determined by preparing a 50 μM solution of **1-3** in MilliQ water and adding an equal volume of 1-octanol.² The UV-vis spectra (350 nm) was taken of the water layer before (*t* = 0) and after diffusion equilibrium (*t* = 15 h) (**Figure S4**). The larger the log *P* value, the higher the solubility in the hydrophobic solvent. The log *P* was calculated by the following:

$$\text{Log } P = [(\text{Abs before} - \text{Abs after})/\text{Abs after}]$$

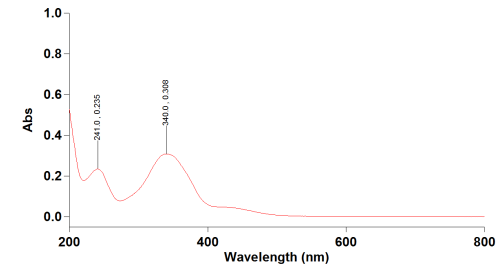
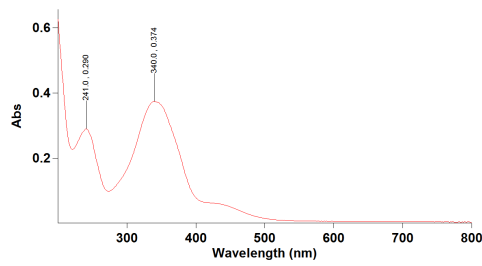
Table S1. Photocontrollable critical micelle concentrations (CMCs, mM), thermal half-life (h) at 20 °C ($t_{1/2(cis)}$) and 1-octanol/water partition coefficients ($\log P$) of surfactants **1-3**.

Surfactant	CMC _{vis}	CMC _{UV}	$t_{1/2}$	$\log P_{vis}$	$\log P_{UV}$
GlcAzo 1 ¹⁷	0.21	0.45	N.D	-0.94	N.D
ManAzo 2	0.23	0.49	23	-0.67	N.D
GalAzo 3	N.D	N.D	N.D	-0.35	-0.85

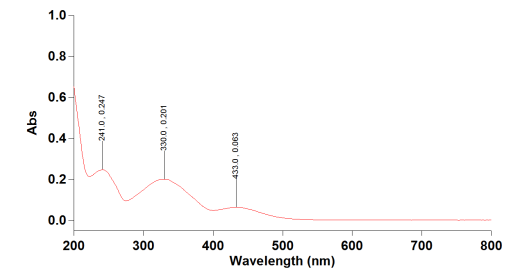
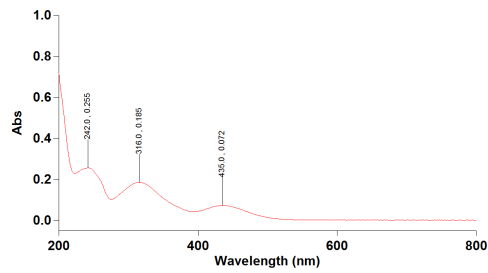
GlcAzo1 (trans)



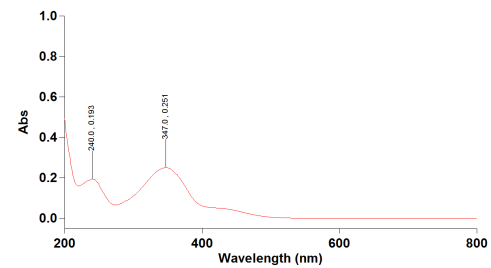
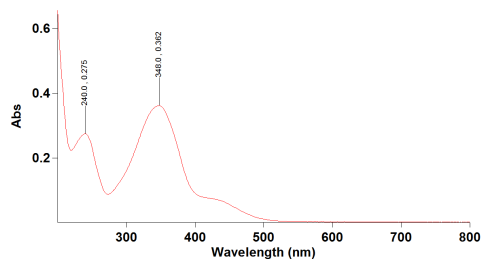
ManAzo 2 (trans)



ManAzo 2 (cis)



GalAzo 3 (trans)



GalAzo 3 (cis)

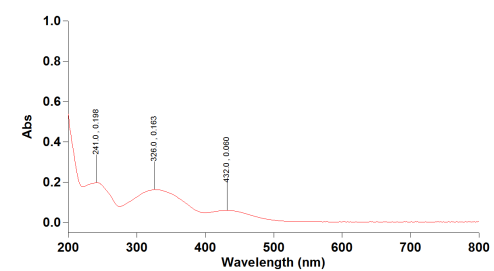
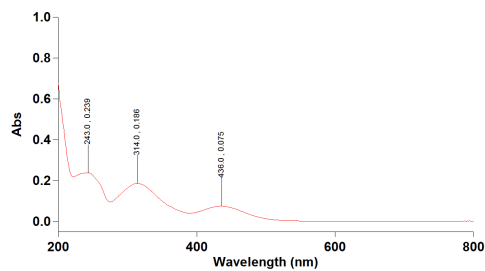


Figure S4. UV-vis spectra of surfactants **1-3** before and after diffusion equilibration in 1:1 v/v water/1-octanol water.

Ice Recrystallization Inhibition (IRI) Assay

To assess ice recrystallization inhibition (IRI) activity, the “splat cooling” method was used.³ The sample was dissolved in a phosphate buffered saline (PBS) solution. Using a micropipette, a 10 μ L droplet of the solution was dropped through a two-meter high plastic tube, having a 10 cm diameter, onto a polished aluminum block cooled to approximately -80 °C with dry ice. The droplet froze immediately upon contact with the surface of the aluminium block, creating a wafer approximately 1 cm in diameter and 20 μ m thick. Using precooled tools, the wafer was separated from the surface of the block and transferred to a cryostage, kept at -6.4 °C. The wafer was annealed for 30 minutes, and then photographed between crossed polarizing filters using a digital camera (Nikon CoolPix 5000) fitted to a microscope. A programmable Peltier unit (S3 Series 800 temperature controller, Alpha Omega Instruments) was used to maintain the temperature of the cryostage. Three images were taken from each wafer. During flash freezing, small ice crystals from the solution are formed very quickly, and during annealing, the ice crystals dramatically increase in size due to recrystallization. In order to quantitatively measure the difference in recrystallization inhibition of two compounds, the difference in the dynamics of ice crystal size distribution was examined. This was done using a novel domain recognition software (DRS)²² program to analyze the image of the ice wafer. From this, domain areas from each image were calculated and data was inputted into Microsoft Excel. Using Microsoft Excel, the data was then plotted and analyzed. The ice crystal mean grain size (MGS) of the sample was compared to the MGS of the PBS control for the same day of testing and IRI activity was reported as percent mean grain size (%MGS). Error bars indicate the standard error of the mean. Each compound was performed in triplicate. In GraphPad, significant difference was determined using the unpaired Student’s T test ($P < 0.05$).

Quantitative Analysis of Ice Recrystallization Inhibition (IRI)

To quantify ice recrystallization inhibition (IRI) activity, a modified “splat cooling” assay (described above) was employed.⁴ Five concentrations (1, 5, 10, 20, 30 mM) of ManAzo were tested in triplicate as well as the PBS control. Instead of a 30-minute annealing period, the wafer was annealed for 5 minutes at -6.4 °C, and then photographed between crossed polarizing filters using a digital camera (Nikon CoolPix 5000) fitted to the microscope. One image was selected from each wafer for further analysis. Using ImageJ, ice crystals with well-defined boundaries within the image were circled, and the area of each circled ice crystal was calculated. Using Excel, the ice crystal areas were sorted into discrete bins based on size (bin size increased in increments of 0.001 mm²). At time zero, all ice crystals could be contained within a bin size of 0.001 mm², and therefore, as crystals grew due to recrystallization, they moved out of bin 1 and into higher bins. The proportionate area of each bin was calculated for each sample wafer by adding the area of each crystal within a bin and dividing by the sum of the areas of all crystals in the image. The rate constants were determined for each inhibitor concentration tested and normalized based on the average rate constant determined for the PBS control (zero inhibitor concentration). Using GraphPad, a dose-response curve was generated using the normalized rate constants, v_{norm} , for each inhibitor concentration, [I], and the corresponding log values of the concentration. A two-parameter sigmoidal curve was fit to the data to obtain the half maximal inhibition concentration (IC₅₀). Error was reported as the standard error of the mean.

Thermal Hysteresis (TH) Assay

Nanoliter osmometry, using a Clifton nanoliter osmometer (Clifton Technical Physics, Hartford, NY), was performed in order to assess the TH activity and dynamic ice shaping (DIS) ability of ManAzo.⁵ In this assay, a single droplet of an aqueous solution (milli q water) of compound was enclosed within an oil-filled well in a sample holder. Using a thermoelectrically-controlled microscope

stage, the sample was frozen and then slowly thawed until a single ice crystal remained. At this point, the morphology of the single ice crystal was monitored, (**Figure S5**) as the temperature of the sample was gradually decreased, through a Leitz compound microscope equipped with an Olympus 20X objective, a Leitz Periplan 32X photo eyepiece, and a Hitachi KPM2U CCD camera connected to a Toshiba MV13K1 TV/VCR system. Non-uniform ice crystal growth is indicative of dynamic ice shaping (DIS) and TH activity is measured as the depression of the freezing point in relation to a static melting point. Due to the amphiphilic nature of ManAzo, a 10 mg mL⁻¹ solution dissolved into the oil phase, creating a single phase. As a result, the TH and DIS activity was assessed at 0.5 mg mL⁻¹. At this concentration, ManAzo did not exhibit DIS nor TH activity.

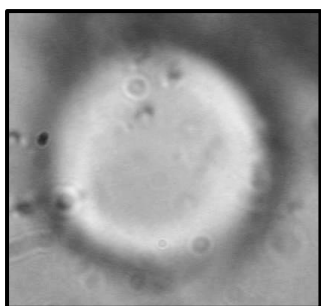


Figure S5. Ice crystal habit in the presence of 0.5 mg mL⁻¹ *trans* ManAzo **2**. The ice crystal grew uniformly in a circular fashion as the temperature was incrementally decreased. The image was taken with a Nikon CoolPix 5000 digital camera.

Cryopreservation of Tf-1 α cells

In order to investigate the cryoprotective ability of ManAzo, **2** Tf-1 α cells were cryopreserved with a 30 mM concentration of the surfactant in 0%, 2%, 5%, 10% DMSO solutions; with controls performed in duplicate and each test concentration performed in triplicate. Error bars represent the percent standard error of the mean. TF-1 α cells (human bone marrow erythroblasts, ATCC CRL-2451) were cultured in RPMI-1640 media supplemented with 1% penicillin-streptomycin and 10% fetal bovine serum (FBS) in 150 mm Corning® petri dishes. Cells were incubated at 37 °C with 5% CO₂. Media

was changed every two days by transferring suspended cells in the culture dish to a 50 mL falcon tube and centrifuging at 1000 rpm for 5 minutes at room temperature. Following this, supernatant was removed and the pellet was re-suspended in RPMI-1640 media by vortex. This was transferred to a new culture dish and 20 mL of media was added. Cells were split if cell count exceeded 5×10^6 cells per plate. Using a hemocytometer, the cell count was obtained by preparing a 1/8 dilution of the cell solution in an eppendorf tube with the dye, trypan blue.

Once enough cells had been cultured (2×10^6 cells/cryovial is required), the contents of the culture dishes were transferred to 50 mL falcon tubes and centrifuged at 1000 rpm for 5 minutes at room temperature. Supernatants were removed and the pellets were re-suspended in a small amount of media. The re-suspended cells were combined into one falcon tube and the total cell count was obtained using a hemocytometer. The volume required to add 2×10^6 cells per cryovial was determined and transferred to each vial. Cryovials were centrifuged at 1000 rpm for 5 minutes at room temperature. Following this, the supernatant was carefully removed, and 100 μ L of the appropriate cryosolution (0%, 2%, 5%, 10% DMSO solutions in media with or without 30 mM ManAzo 2) was added to each vial. Cryovials were vortexed and transferred to a "Mr. Frosty" freezing container and placed in a -80 °C freezer for 18 hours. The cryovials were then placed in a -196 °C storage dewar for a minimum of 12 hours prior to analysis.

Cryovials were thawed under fast-thaw conditions (37 °C water bath) followed by the addition of 900 μ L 1X Annexin V binding buffer to each cryovial. The contents were mixed and 400 μ L of each vial was transferred to eppendorf tubes. 10 μ L 7-AAD and 10 μ L Annexin V FITC were added, and the tubes were incubated in the dark for 15 minutes at room temperature. 20 μ L counting beads were added followed by the addition of 1X Annexin V binding buffer to a total volume of 1 mL. The solutions were filtered into flow tubes prior to flow cytometry. Flow cytometry was performed on a Beckman Coulter

Gallios Flow Cytometer using Kaluza for Gallios as software. Annexin V-FITC was measured with 518 nm optical filter (FL-1), while 7-AAD was measured with 570 nm optical filter (FL-4). Viability (**Figure S6**) was determined as the amount of 7-AAD⁻ cells detected and apoptosis was determined as the amount of 7-AAD⁻ cells that were also Annexin V FITC⁺. Bead counts and total post-thaw cell counts were obtained for each sample. Cell recovery (**Figure S7**) was calculated as the concentration of cells post thaw divided by the pre-freeze cell concentration. The time between thawing and flow cytometry analysis was under 1 hour.

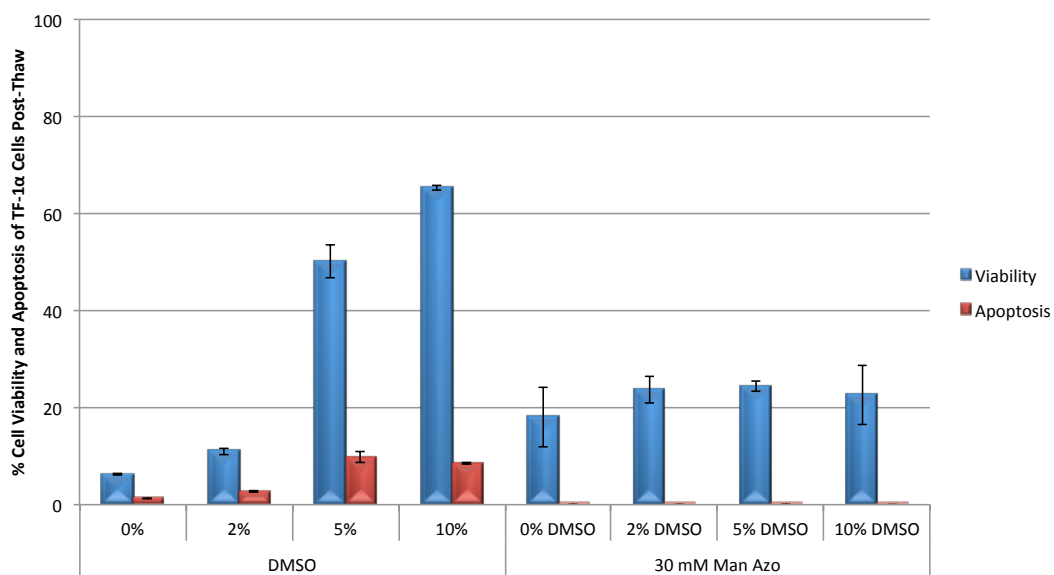


Figure S6. Percent post-thaw cell viability and apoptosis of TF-1 α cells cryopreserved with 30 mM ManAzo 2 in varying concentrations of DMSO.

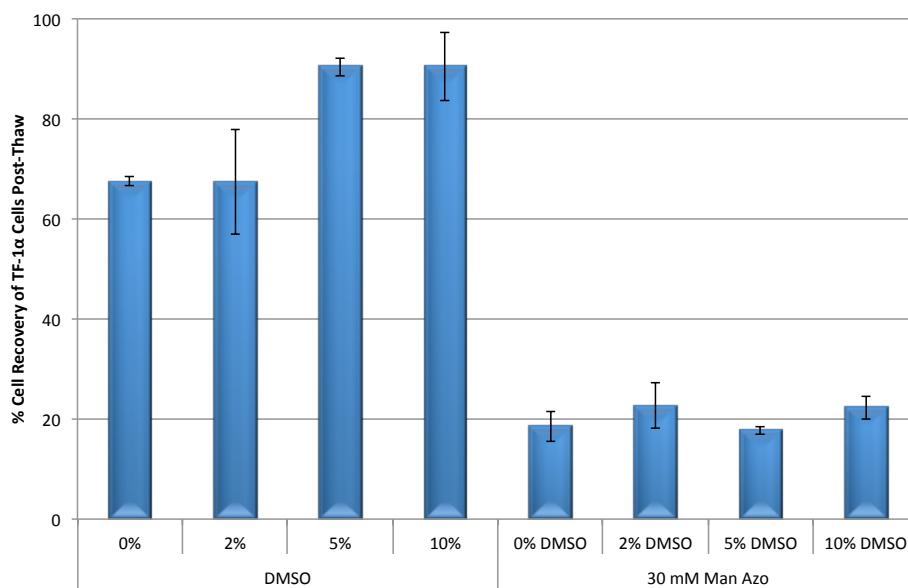


Figure S7. Percent post-thaw cell recoveries of TF-1 α cells cryopreserved with 30 mM ManAzo 2 in varying concentrations of DMSO.

Toxicity Experiments with ManAzo 2 (30 mM)

Each condition was performed in triplicate. Error bars represent the percent standard error of the mean. Cells were cultured as described above. Once enough cells had been cultured (2×10^6 cells/sample is required), the contents of the cultures dishes were transferred to 50 mL falcon tubes and centrifuged at 1000 rpm for 5 minutes at room temperature. Supernatants were removed and the pellets were re-suspended in a small amount of media. The re-suspended cells were combined into one falcon tube and the total cell count was obtained using a hemocytometer. The volume required to add 2×10^6 cells per cryovial was determined and the appropriate amount was transferred to each vial. Cryovials were centrifuged at 1000 rpm for 5 minutes at room temperature. Following this, the supernatant was carefully removed, and 100 μ L of either media or 30 mM ManAzo in media was added to each vial. Cryovials were vortexed and incubated for 30 minutes at 37 °C with 5% CO₂.

900 μ L 1X Annexin V binding buffer was added to each cryovial. The contents were mixed and 400 μ L of each vial was transferred to eppendorf tubes. 10 μ L 7-AAD and 10 μ L Annexin V FITC were added, and the tubes were incubated in the dark for 15 minutes at room temperature. 20 μ L counting beads were added followed by the addition of 1X Annexin V binding buffer to a total volume of 1 mL. The solutions were filtered into flow tubes prior to flow cytometry. Flow cytometry was performed on a Beckman Coulter Gallios Flow Cytometer using Kaluza for Gallios as software. Annexin V-FITC was measured with 518 nm optical filter (FL-1), while 7-AAD was measured with 570 nm optical filter (FL-4). Viability (**Figure S8**) was determined as the amount of 7-AAD⁻ cells detected and apoptosis was determined as the amount of 7-AAD⁻ cells that were also Annexin V FITC⁺. Bead counts and total post-incubation cell counts were obtained for each sample. Cell recovery (**Figure S9**) was calculated as the concentration of cells post-incubation divided by the pre-incubation cell concentration.

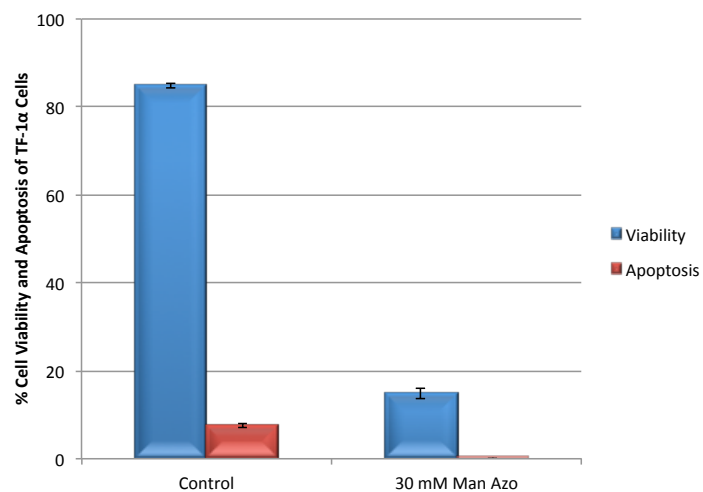


Figure S8. Percent cell viability and apoptosis of TF-1 α cells incubated at 37°C for 30 minutes with or without 30 mM ManAzo **2**.

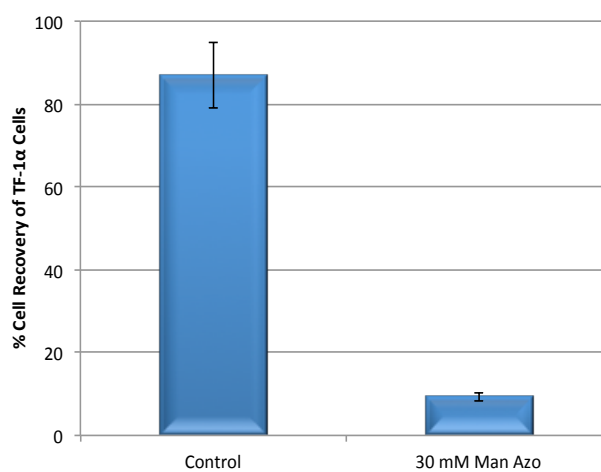
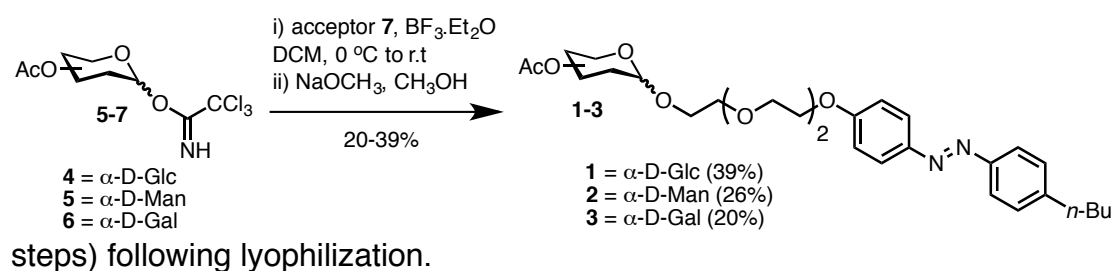


Figure S9. Percent cell recovery of TF-1 α cells incubated at 37°C for 30 minutes with or without 30 mM ManAzo **2**.

2.0 Synthesis and analytical data

General procedure

Carbohydrate surfactants **1-3** were synthesized using an adapted literature procedure (**Scheme S1**).^{1,6} A mixture of the azobenzene acceptor⁷ (1.0 equiv) and per-*O*-acetyl glycosyltrichloroacetimidate (1.5 equiv) in dry DCM at 0 °C under an N₂ atmosphere was added boron trifluoride etherate (1.0 equiv) dropwise. The solution was stirred at 0 °C for 1h, and gradually warmed to room temperature. The reaction was left to stir at r.t for 16 hours, at which time TLC analysis indicated consumption of starting materials and formation of product. The reaction was quenched by the addition of *N,N*-diisopropylethylamine, washed with water, saturated aqueous NaHCO₃ solution and brine. The organic layer was dried (Na₂SO₄), filtered and evaporated to afford a crude oil, which was used in the next step without further purification. The crude residue was re-dissolved in methanol and treated with a 1M NaOCH₃ solution. The reaction was deemed complete following LC-MS analysis. The solution was neutralized with Amberlite IR-120 acidic ion exchange resin, filtered, and concentrated *in vacuo*. The residue was purified by reversed phase preparative HPLC (see general methods for details) to give surfactants **1-3** as bright yellow solid (31-51% yield over two

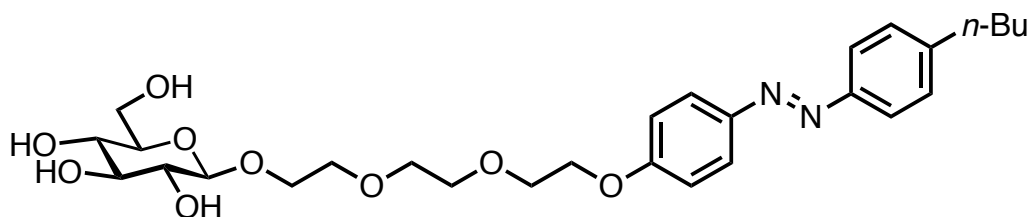


steps) following lyophilization.

Scheme S1. Synthesis of carbohydrate-based photosurfactants **1-3**.

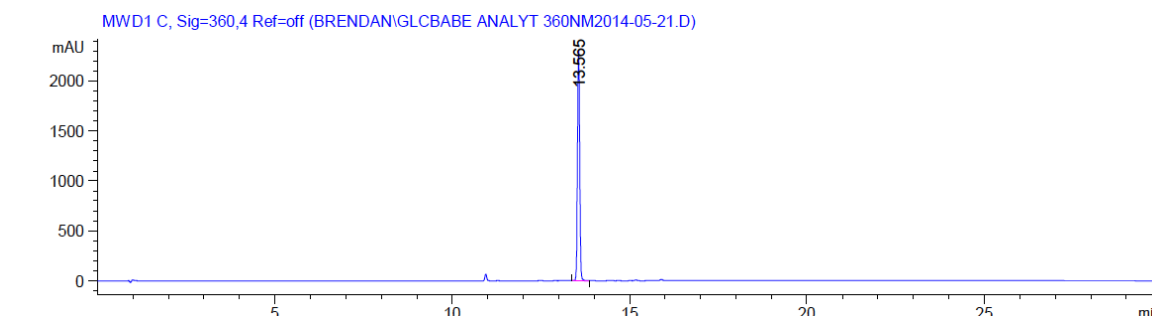
Analytical data

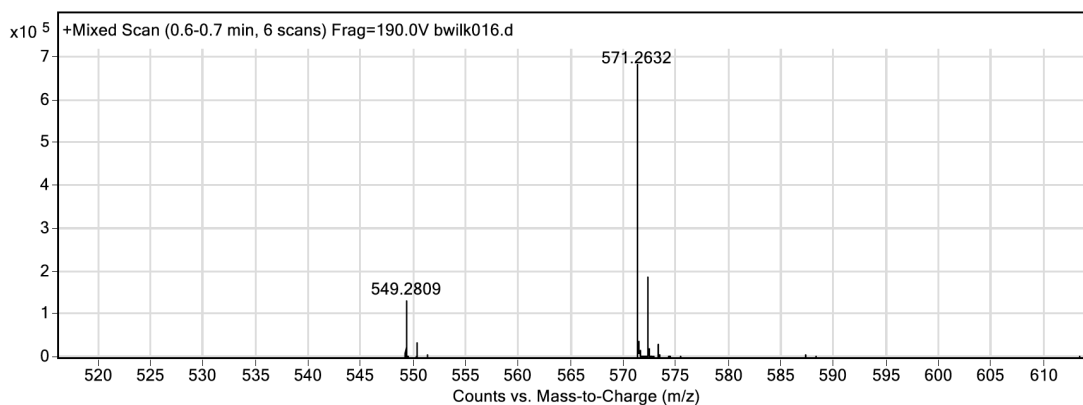
2-[2-[2-(4-*n*-butylazophenyl phenoxy)ethoxy]ethoxy]ethyl α -D-glucopyranoside (GlcAzo) **1**¹



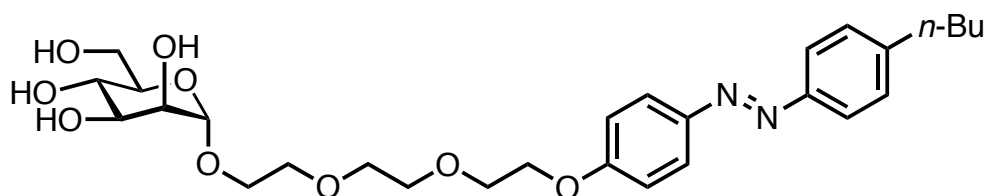
GlcAzo (**1**)

Yield: 39%. Mp = 41.2 °C; $[\alpha]_D^{20}$ -10.5 (*c*, 0.09 in CH₃OH); FT-IR (ATR): ν_{\max} 3355, 2924, 2872, 1596, 1250 cm⁻¹; ¹H NMR (400 MHz, CD₃OD) δ 7.88 (2H, d, *J* = 9.0 Hz), 7.78 (2H, d, *J* = 8.4 Hz), 7.33 (2H, d, *J* = 8.5 Hz), 7.09 (2H, d, *J* = 9.1 Hz), 4.30 (1H, d, *J* = 7.8 Hz), 4.25-4.22 (2H, m), 4.03-3.98 (1H, m), 3.90-3.87 (2H, m), 3.84-3.84 (1H, m), 3.75-3.63 (9H, m), 3.38-3.33 (1H, m), 3.28-3.26 (2H, m), 3.20 (1H, dd, *J* = 9.1, 7.8 Hz), 2.70 (2H, t, *J* = 7.7 Hz), 1.69-1.62 (2H, m), 1.45-1.35 (2H, dq, *J* = 14.9, 7.4 Hz), 0.96 (3H, t, *J* = 7.4 Hz); ¹³C NMR (100 MHz, CD₃OD) δ 162.7, 152.3, 148.3, 147.2, 130.1, 125.6, 123.5, 116.0, 104.4, 77.9, 75.0, 72.4, 71.7, 71.6, 71.5, 71.4, 70.7, 69.6, 68.9, 62.7, 43.8, 36.4, 34.7, 23.3, 14.3. LC-MS: *m/z* 549.1 [*M* + H]⁺, 571.0 [*M* + Na]⁺. HRMS (ESI-ToF) calculated for C₂₈H₄₁N₂O₉ 549.2812 [*M* + H]⁺, found 549.2809 [*M* + H]⁺



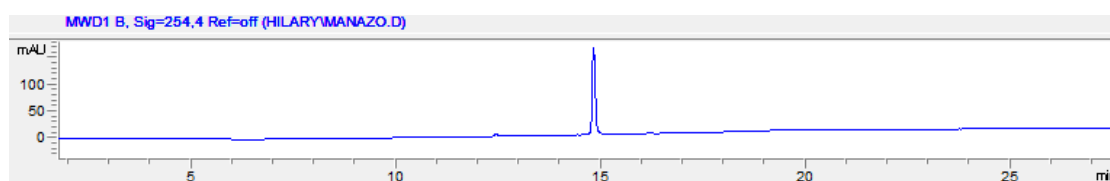


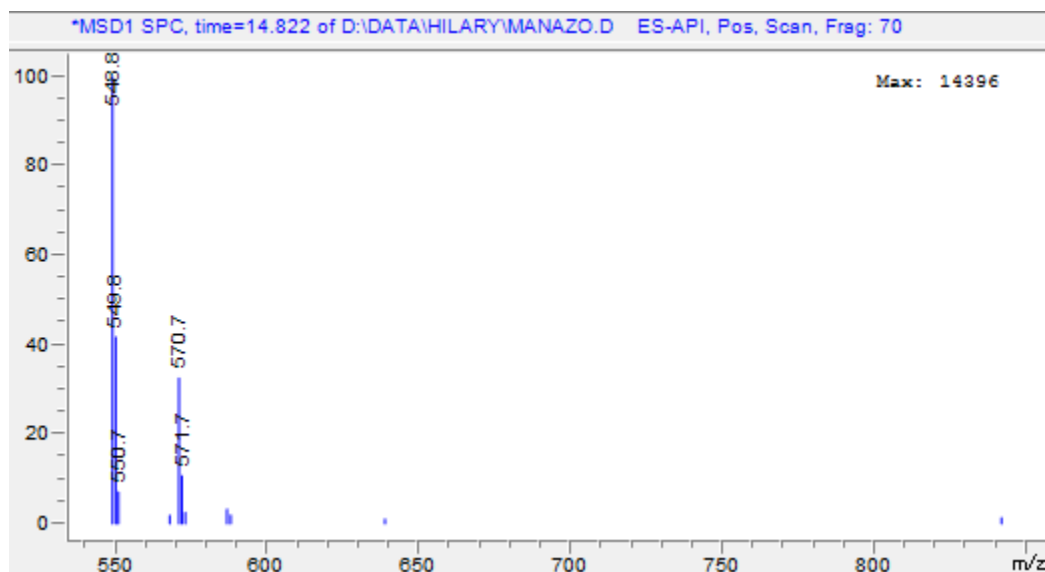
2-[2-[2-(4-*n*-butylazophenyl phenoxy)ethoxy]ethoxy]ethyl α -D-mannopyranoside (ManAzo) **2**



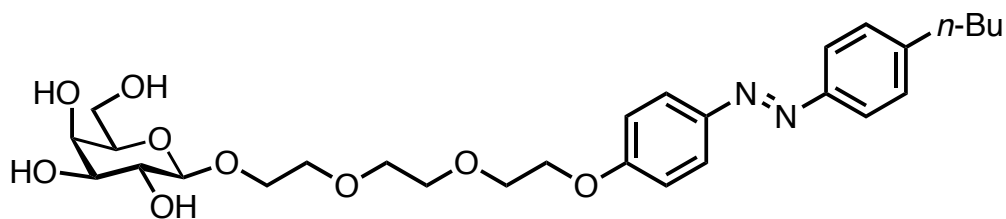
ManAzo (**2**)

Yield: 26% Mp = 191.2 °C (decomp); $[\alpha]_D^{20} +27.3$ (c, 0.003 in CH₃OH); FT-IR: $\nu_{\max}/\text{cm}^{-1}$ 3297, 2929, 2877, 1576, 1498, 1412, 1248, 1051, 840, 648; ¹H NMR (400 MHz, CD₃OD) δ 7.87 (2H, d, $J=9.07\text{Hz}$), 7.77 (2H, d, $J=8.35\text{Hz}$), 7.32 (2H, d, $J=8.38\text{Hz}$), 7.08 (2H, d, $J=9.06\text{Hz}$), 4.82-4.79 (1H, m), 4.23-4.20 (2H, m), 3.89-3.56 (17H, m), 2.68 (2H, t, $J=7.66\text{Hz}$), 1.67-1.60 (2H, m), 1.43-1.34 (2H, m), 0.95 (3H, t, $J=7.33\text{Hz}$); ¹³C NMR (400 MHz, CD₃Cl₃) δ 161.4, 150.9, 146.9, 145.9, 128.8, 124.2, 122.2, 114.6, 100.3, 73.2, 71.1, 70.7, 70.4, 70.2, 70.0, 69.4, 67.6, 67.1, 66.4, 61.3, 35.1, 33.4, 22.9, 21.9, 12.9. LC-MS: m/z 548.8 [$M + H$]⁺, 570.7 [$M + Na$]⁺, HRMS (ESI-ToF) calculated for C₂₈H₄₀N₂O₉ 548.2734 [$M + H$]⁺, found 571.2621 [$M + Na$]⁺





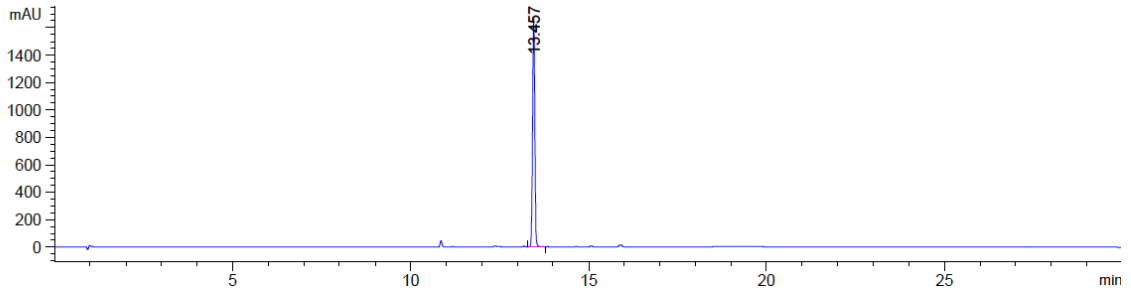
2-[2-[2-(4-*n*-butylazophenyl phenoxy)ethoxy]ethoxy]ethyl α -D-galactopyranoside (GalAzo) **3**¹



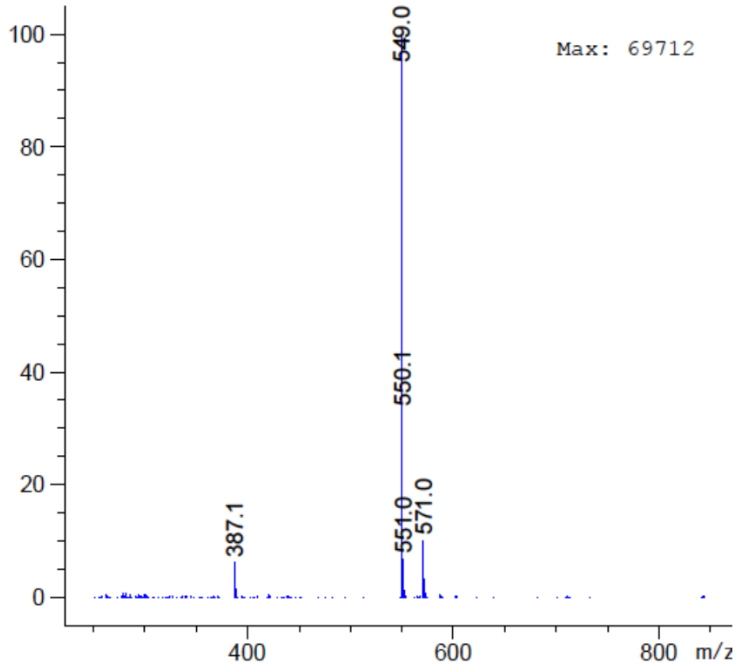
GalAzo (**3**)

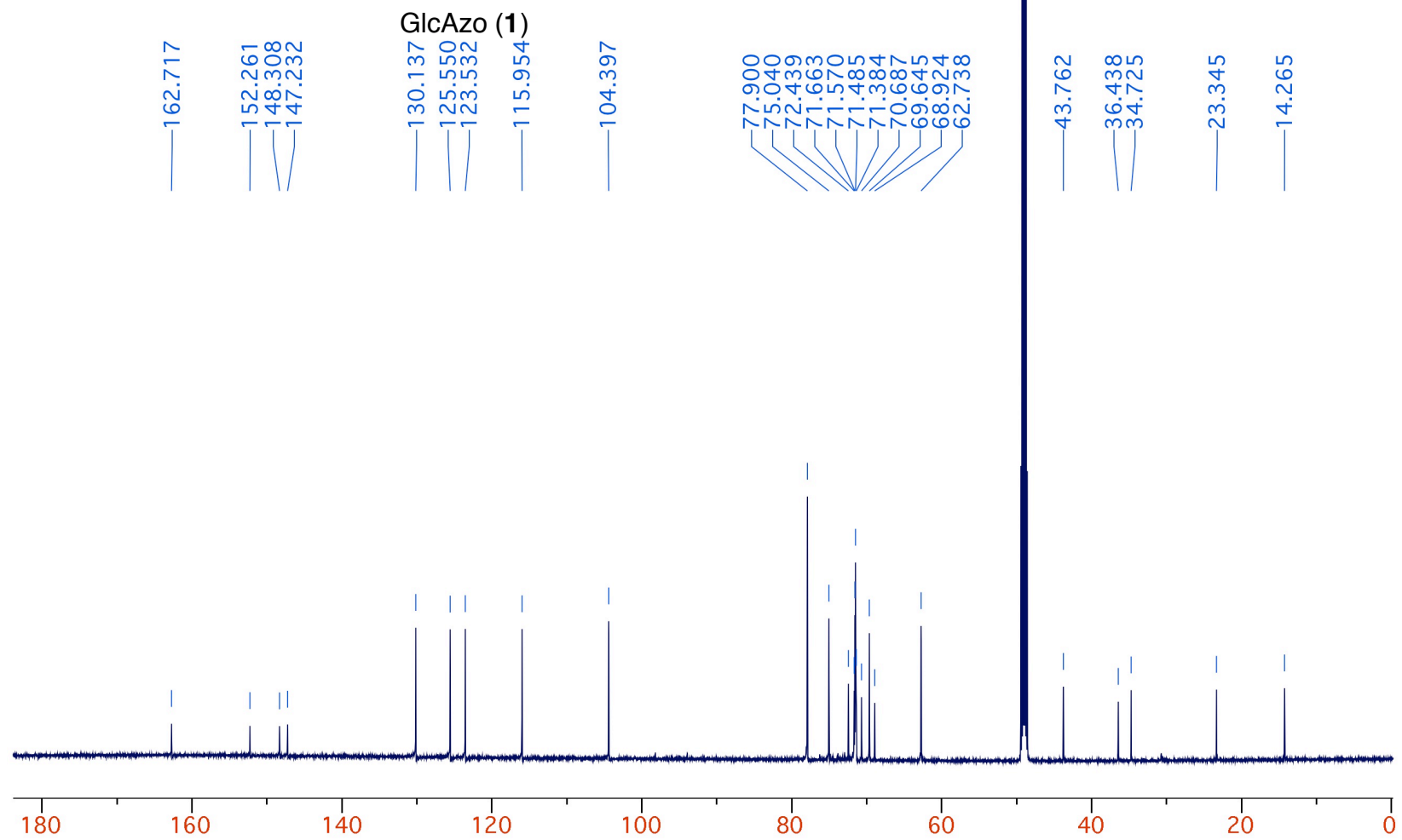
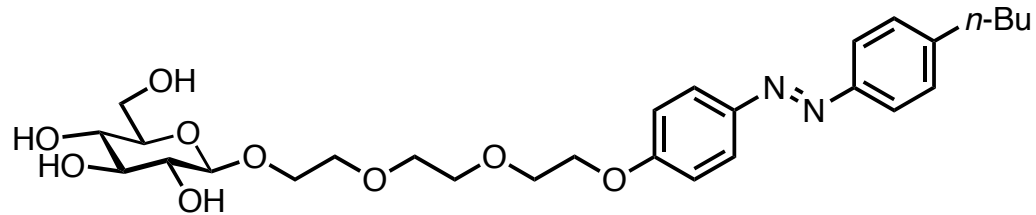
Yield: 20%. Mp = 43.4 °C; $[\alpha]_D^{20} - 6.0$ (c, 0.08 in CH₃OH); ¹H NMR (400 MHz, CD₃OD) δ 7.88 (2H, d, $J = 9.1$ Hz), 7.78 (2H, d, $J = 8.4$ Hz), 7.34 (2H, d, $J = 8.6$ Hz), 7.10 (2H, d, $J = 9.1$ Hz), 4.26-4.23 (3H, m), 4.03-3.98 (1H, m), 3.90-3.87 (2H, m), 3.80 (1H, dd, $J = 3.3, 0.9$ Hz), 3.78-3.69 (10H, m), 3.55-3.44 (4H, m), 2.70 (2H, t, $J = 7.7$ Hz), 1.70-1.62 (2H, m), δ 1.40 (2H, m), 0.97 (3H, t, $J = 7.4$ Hz); ¹³C NMR (100 MHz, CD₃OD) δ 162.7, 152.2, 148.2, 147.3, 130.3, 125.7, 123.6, 116.1, 105.1, 76.6, 74.9, 72.4, 72.3, 71.6, 71.5, 71.4, 70.6, 70.1, 69.5, 69.0, 62.4, 44.2, 36.7, 34.7, 23.3, 14.4; LC-MS: m/z 549.0 [$M + H$]⁺, 571.0 [$M + Na$]⁺; HRMS (ESI-ToF) calculated for C₂₈H₄₁N₂O₉ 549.2812 [$M + H$]⁺, found 549.2808 [$M + H$]⁺

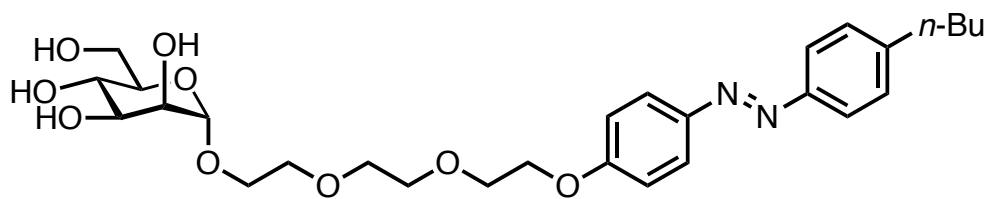
MWD1 C, Sig=360,4 Ref=off (BRENDANIGALBABE ANALYT 360NM2014-05-21.D)



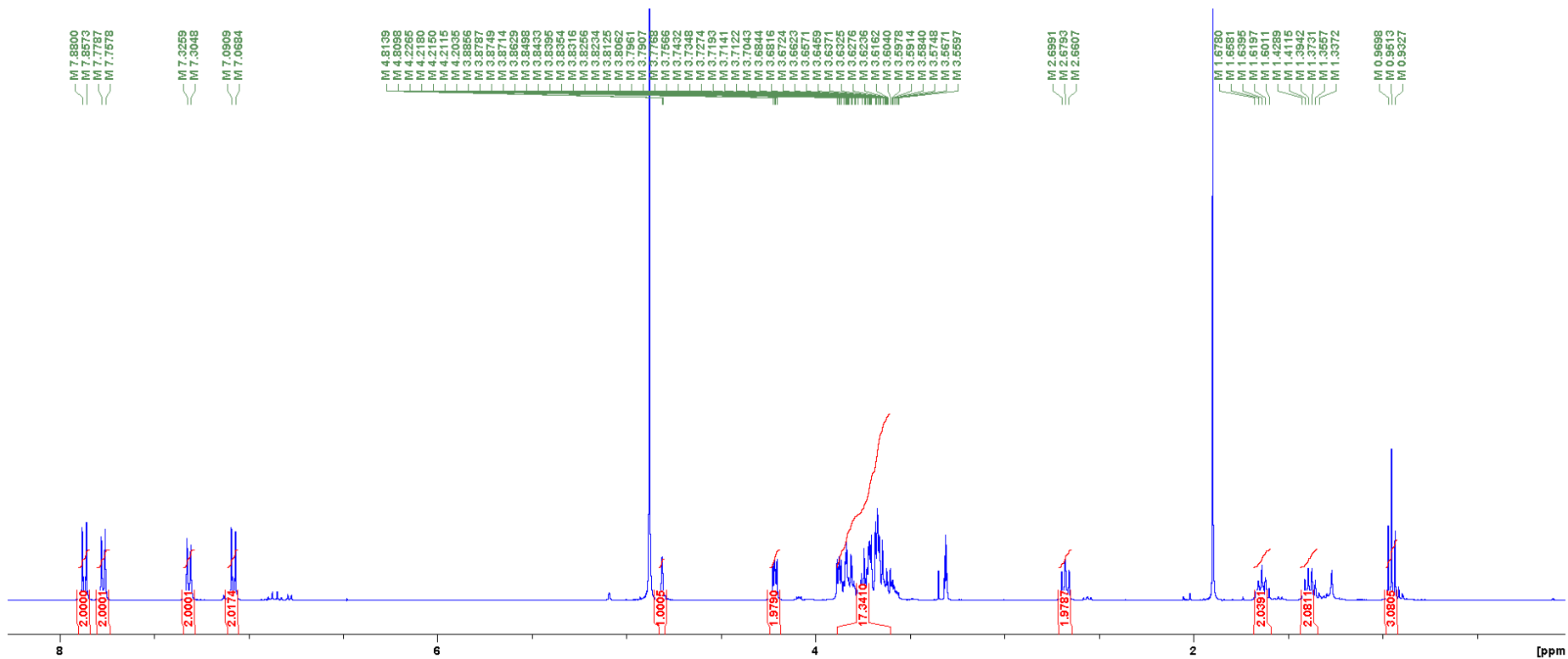
*MSD1 SPC, time=13.411:14.307 of D:\DATA\BRENDAN\GALBAE

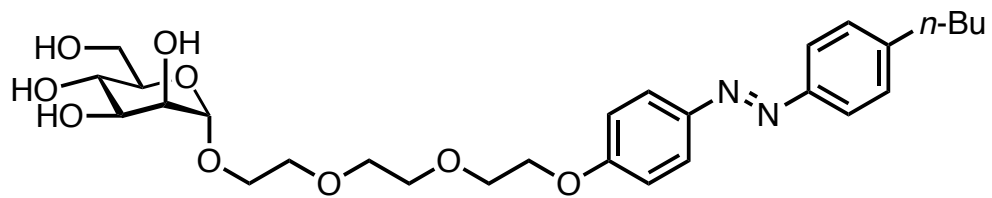




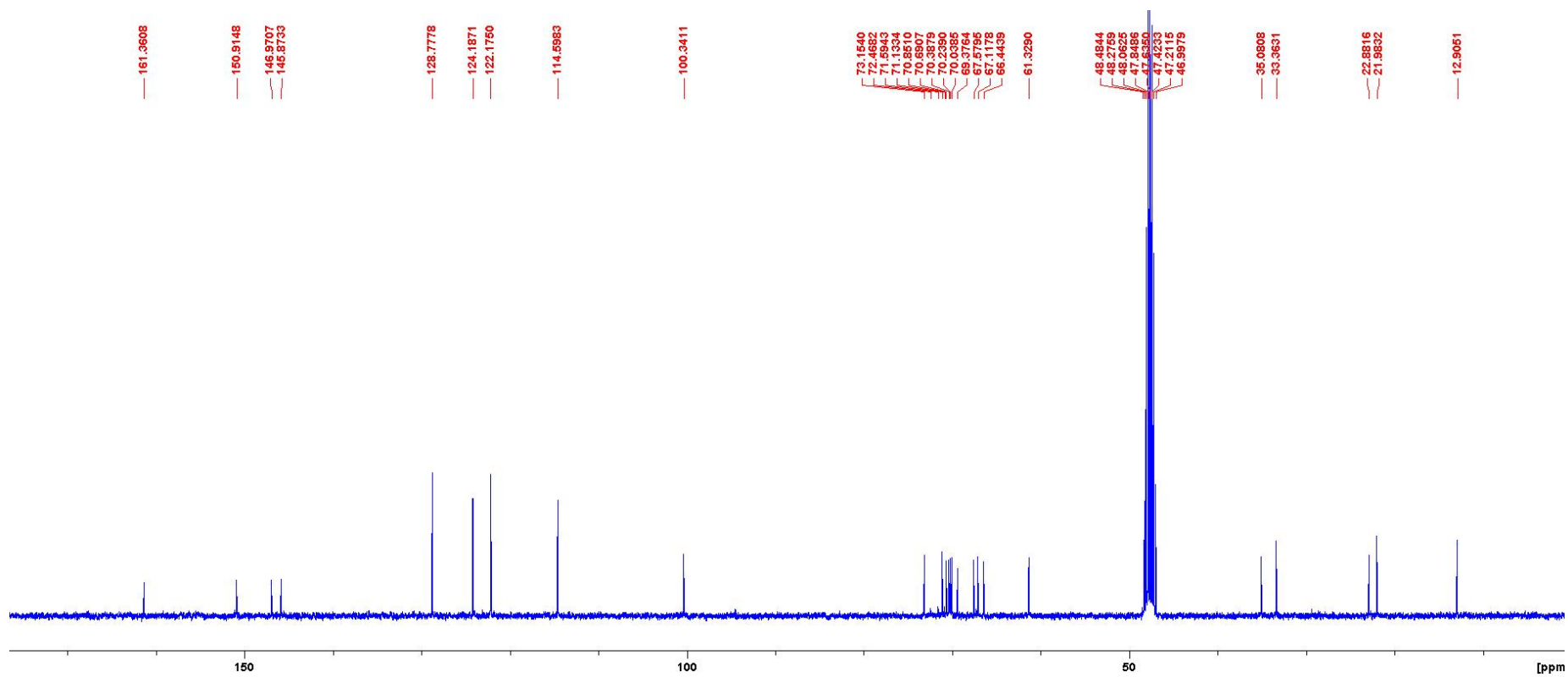


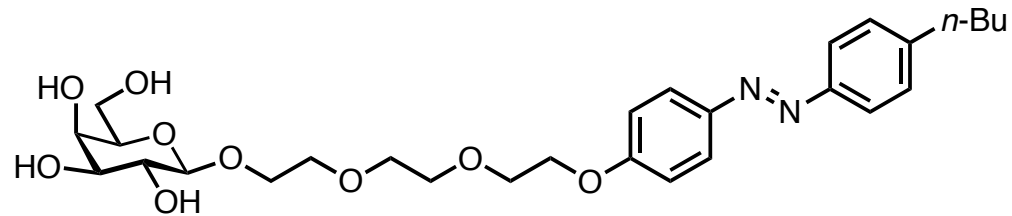
ManAzo (2)



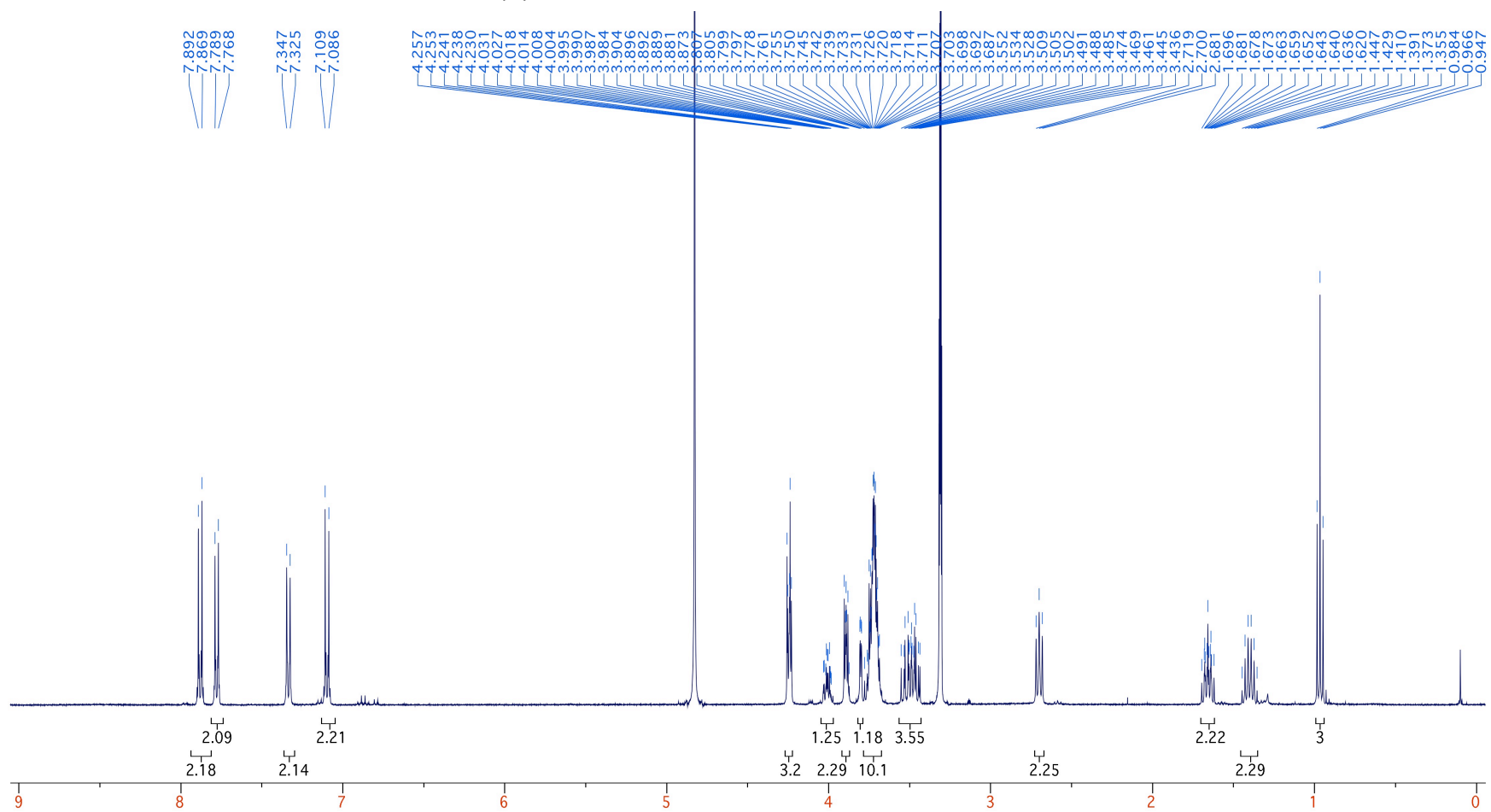


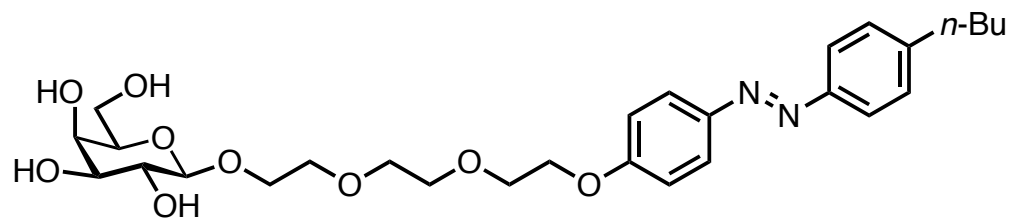
ManAzo (2)



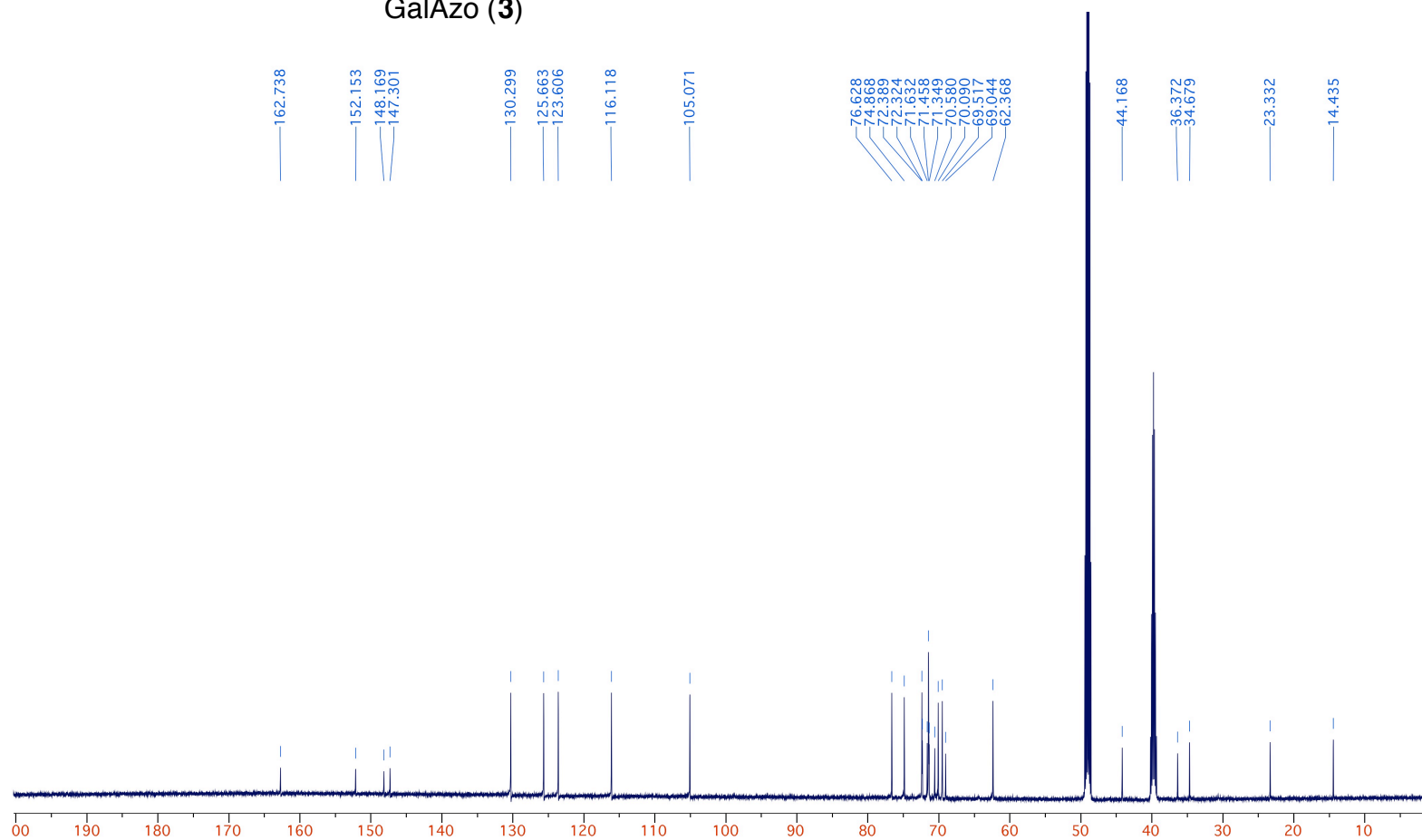


GalAzo (3)





GalAzo (3)



3.0 References

- 1) R. F. Tabor, D. D. Tan, S. S. Han, S. A. Young, Z. L. E. Seeger, M. J. Pottage, C. J. Garvey, B. L. Wilkinson, *Chem.-Eur. J.* 2014, **20**, 13881.
- 2) Y. Hu, J. B. Marlow, R. Ramanathan, W. Zou, H. G. Tiew, M. J. Pottage, V. Bansal, R. F. Tabor, B. L. Wilkinson, *Aust. J. Chem.* 2015, **68**, 1880.
- 3) C. A. Knight, J. Hallett, A. L. DeVries. *Cryobiology*, 1988, **25**, 55.
- 4) S. Abraham, K. Keillor, C. J. Capicciotti, G. E. Perley-Robertson, J. W. Keillor, R. N. Ben, *Cryst. Growth Des.* 2015, **15**, 5034.
- 5) A. Chakrabarty, C. L. Hew, *Eur. J. Biochem.* 1991, **202**, 1057.
- 6) G. T. Noble, S. L. Flitsch, K. P. Liem, S. J. Webb, *Org. Biomol. Chem.* 2009, **7**, 5245.
- 7) M. Billamboz, F. Mangin, N. Drillaud, C. Chevrin-Villette, E. Banaszak-Léonard, C. Len, *J. Org. Chem.* 2014, **79**, 493.